ASIAN JOURNAL OF PHARMACEUTICAL AND CLINICAL RESEARCH

INNOVARE ACADEMIC SCIENCES
Knowledge to Innovation

Vol 14, Issue 12, 2021

Online - 2455-3891
Print - 0974-2441

Research Article

PHYTOSYNTHESIS AND CHARACTERIZATION OF SILVER NANOPARTICLES FROM *RUELLIA TUBEROSA* (L.): EFFECT OF PHYSICOCHEMICAL PARAMETERS

HARIKA M, RADHIKA P*

Department of Biochemistry, Andhra University, Visakhapatnam, Andhra Pradesh, India. Email: parvataneni_radhika@yahoo.com

Received: 11 March 2021, Revised and Accepted: 06 November 2021

ABSTRACT

Objective: The current study focused on synthesizing silver nanoparticles (AgNPs) using *Ruellia tuberosa* aqueous tuber extract (RTTE) and silver nitrate ($AgNO_3$) solution.

Methods: AgNPs were synthesized using an aqueous tuber extract of the medicinal herb *R. tuberosa* (L.). The existence of significant phytoconstituents involved in synthesizing the AgNPs was determined using the gas chromatography–mass spectrometry (GC–MS) study. We evaluated the physical and chemical parameters such as the effect of time, temperature, metal ion concentration, crude aqueous tuber extract concentration, and pH in the synthesis of nanoparticles. The AgNPs were characterized using ultraviolet (UV)–Vis spectroscopy, field emission scanning electron microscopy (FESEM), energy-dispersive X-ray spectroscopy (EDX), high-resolution transmission electron microscope (HRTEM), selected area electron diffraction (SAED), X-ray diffraction (XRD), and Fourier transform infrared (FTIR) techniques.

Results: *R. tuberosa* tuber extract was rich in various phytochemical constituents which were identified by GC–MS. For biosynthesis, the optimal values were 1 mM $AgNO_3$concentration, 0.1 mL of aqueous tuber extract, and a 40 min incubation temperature of 70°C. The existence of a characteristic surface plasmon resonance (SPR) peak at 421 nm indicated the biosynthesis of AgNPs using UV–Vis spectroscopy. At higher temperatures and alkaline pH, the development of AgNPs increased overtime and remained stable up to 4 weeks. FESEM, EDX, HRTEM, SAED, and XRD analysis revealed that most AgNPs were spherical, with an average size distribution of 34.9 nm and a crystalline phase, face-centered cubic lattice. Infrared (FTIR) spectroscopic analysis revealed that hydroxyl and amino functional groups were involved in the biosynthesis and stabilization of AgNPs.

Conclusion: The synthesis of AgNPs from *R. tuberosa* aqueous tuber extract was a cost-effective process and environmental friendly.

Keywords: *Ruellia tuberosa*, Silver nanoparticles, Ultraviolet–visible spectroscopy, High-resolution transmission electron microscope, X-ray diffraction.

 DOI: http://dx.doi.org/10.22159/ajpcr.2021v14i12.42020. Journal homepage: https://innovareacademics.in/journals/index.php/ajpcr

INTRODUCTION

In the field of nanobiotechnology, there had been significant advancements in recent years. Materials classified as nanoscaled structures usually had one dimension less than 100 nm. Relative surface area and size were the two main factors that influenced the chemical reactivity, electrical, optical, and thermal properties of nanoparticles [1]. Metal nanoparticles such as silver, gold, palladium, zinc, copper, and iron oxide were synthesized using a variety of physical, chemical, and biological methods [2-4]. A variety of metal nanoparticles were synthesized using biological agents such as plants and their pure compounds, algae, bacteria, fungi, and yeast. In the case of microorganisms, however, the intricate process of maintaining cell culture was complicated [5,6].

Silver nanoparticles (AgNPs) were synthesized from live alfalfa plants (*Medicago sativa*) intracellularly [7]. The plant extracts of *Indigofera tinctoria*, *Curcuma zedoaria*, *Astragalus tribuloides*, *Clinacanthus nutans*, and *Eriobotrya japonica* served as green reactants in AgNPs synthesis [8-12]. Many researchers currently focused on nanoparticles synthesized using medicinal plants and their various biological efficacies such as antimicrobial, antimalarial, antiviral, anticancer, and antidiabetic [1,10,13,14].

Ruellia tuberosa L. was a low-growing perennial herb with tuberous roots in the *Acanthaceae* family. *R. tuberosa*, a native of America, had a common name, Minnie root, popping pod. Tuber powder was given with milk to treat abdominal pain after delivery [15]. This plant's roots had been used to reduce toxicity and promote healing in cases of urinary tract inflammation [16]. The reported biological activities of the plant's tubers were antioxidant, antispermatogenic, anti-inflammatory, and antimicrobial [17-20]. Previously, there was a report on synthesis of silver and iron oxide nanoparticles from leaf extracts of *R. tuberosa* [20,21]. In this present study, *R. tuberosa* aqueous tuber extract (RTTE) was used to synthesize AgNPs and to study their antiproliferative activity for the 1st time.

MATERIALS AND METHODS

Materials

Silver nitrate ($AgNO_3$) was purchased from HiMedia, Mumbai, India. All the other chemicals and reagents used for the experiments were analytical grades obtained from HiMedia and Sigma-Aldrich, India.

Collection of plant materials

R. tuberosa tubers were collected from the Biodiversity Park, Visakhapatnam, India. The plant was authenticated and identified by Prof. B. Padal (voucher specimen no.22235) at the Herbarium Department of Botany, Andhra University, Visakhapatnam, India.

Preparation of tuber extract

About 15 g (fresh tubers, wet weight) of tubers were measured, washed thoroughly with water, and then again washed with distilled water to remove dust particles. The mashed tubers were blended with 50 mL Milli-Q water and boiled for 15 min. The extract was filtered twice with Whatman no.1 filter paper. The aqueous tuber extract had a pH of 7.5. This extract was stored at 4°C for future work. The tubers of *R. tuberosa* were collected, washed thoroughly in tap water, shade

dried, and powdered in a blender for gas chromatography–mass spectrometry (GC–MS) analysis. The respective plant tuber powder, approximately 70 g of dry weight, was filled in the thimble and extracted successively with ethanol using a Soxhlet extractor. A rotary flash evaporator was used to concentrate the extracts, which were then stored at 4°C.

Phytochemical evaluation of both aqueous tuber extract and ethanolic extracts was done to determine the active phytoconstituents such as alkaloids, phenolics, flavonoids, steroids, terpenoids, saponins, coumarins, carbohydrates, cardiac glycosides, amino acids, and protein compounds using standard methods [22].

GC–MS analysis of *R. tuberosa*

A GC–MS analysis was used to investigate the phytochemical constituents of an ethanolic extract of *R. tuberosa.* Thermo GC-TRACE ultraversion 2.2, Thermo TSQ QUANTUM XLS (Thermo Scientific Co.). The following were the GC–MS system's experimental conditions: Dimensions: 30 Mts, ID: 0.25 mm, film thickness: 0.25 µm, DB 5-MS capillary standard non-polar column. The mobile phase flow rate was set to 1.0 mL/min (carrier gas: He). In the gas chromatography section, the oven temperature was 40°C, which was gradually increased to 290°C at a 5°C/min rate, and the injection volume was 1.0 L. A scan interval of 0.5 s was used to maintain a range of 40–600 m/z. The GC took 35 min to complete. The compounds were identified by comparing their mass spectra to those of the WILEY and NIST libraries.

Synthesis of AgNPs

$AgNO_3$ in Milli-Q water was used as a source of silver. All the experiments were done in duplicates. Synthesis of AgNPs was carried out at 70°C in a boiling water bath by taking a standard reaction mixture contains 1 mL of RTTE in 8 mL of 1 mM $AgNO_3$. At room temperature, various optimization studies were carried out to determine the optimal reaction ratio (1:1, 1:2, 1:4, 1:6, 1:8, 1:10, 1:12, and 1:14) for AgNP formation and to study their stability [23]. The golden yellow color in the reaction mixtures (1:10, 1:12, and 1:14) was taken as the primary indicator of AgNP synthesis. Even after 20 h, the ratios 1:1, 1:2, 1:4, 1:6, and 1:8 did not achieve the same level of color transition. This significant time lag showed that AgNPs need additional energy for bioreduction.

Study of the effect of physicochemical parameters on AgNPs synthesis

The extract concentration was 0.1 mL, and the $AgNO_3$ concentration was 0.8 mL to form reaction mixture (1:8). The effect of temperature on nanoparticle synthesis was investigated by incubating the reaction mixture at various temperatures (40°, 50°, 60°, 70°, 80°, 90°, and 100°C). The effect of metal ions was also monitored by adjusting the $AgNO_3$ concentration (1, 2, 3, 4, and 5 mM) with a constant volume of aqueous tuber extract. By keeping 1 mM $AgNO_3$ at a constant range, the effect of crude aqueous tuber extract concentration (0.1, 0.2, 0.3, 0.4, and 0.5 mL) was analyzed. The effect of pH (4–12) on nanoparticle synthesis investigated using different buffers. In addition, stability studies were carried out in the presence or absence of a stabilizing agent. Following the study, the optimum concentration was chosen for bulk nano colloid preparation. Centrifugation at 10,000 rpm for 15 min was done to extract AgNPs. The pellet was redispersed 2–3 times in Milli-Q water. Further, the characterizations were carried out on the dried nanoparticles.

Characterization of AgNPs

The biosynthesis of AgNPs was first confirmed using ultraviolet (UV)–Vis spectroscopy (SHIMADZU, UV-1800) in the range of 300–700 nm. In order to measure the characteristic optical properties of AgNPs in the colloidal reaction mixture. Field emission scanning electron microscopy (FESEM) (JOEL, JSM-7100F) was used to determine the particle morphology at a 6 kV accelerating voltage. Carbon tape was coated with AgNPs, which were then marked. Energy-dispersive X-ray spectroscopy (EDX), which was connected with FESEM, was used to determine the purity of the AgNPs. The morphology of the synthesized AgNPs was further investigated using a high-resolution transmission electron microscope (HRTEM) on a Tecnai G2, F30 HRTEM 300 kV. For HRTEM analysis, a drop coating of ultrasonically scattered AgNPs was applied to the transmission electron microscope (TEM) grid and dried under UV light. HRTEM images were analyzed with the "image J" tool to determine the average particle size distribution. An X-ray diffractometer analysis was also used to conduct X-ray diffraction (XRD) (Panalytical, X-Pert pro, and Netherland) analysis. The functional groups involved in AgNP biosynthesis and stability were screened using Fourier transform infrared (FTIR) spectroscopy in the range of 4000–400 cm^{-1} using Bruker (ALPHA-T) IR by KBr pelleting.

Antiproliferative activity using sulforhodamine B assay

For the present study, five human cancer cell lines (A549, HeLa, MDA-MB 231, PANC-1, and SK-OV-3) were selected. The National Centre for Cell Sciences in Pune, India, provided the cell lines. The cells were maintained in Dulbecco's modified eagle medium, minimal essential medium, and Roswell Park Memorial Institute Medium with glutamine, and were passaged using conventional trypsinization. In a 96-well plate, cells were plated at a density of about 10,000 cells per well. Cells were treated with different concentrations of RTAgNPs (10, 20, 40, 60, 80, and 100 µg/ml) in triplicates for potent compounds and incubated for 48 h. After the incubation time, cell monolayers were fixed in a 10% trichloroacetic acid solution at 4°C for 1 h, after which the cells were washed with Milli-Q water to extract the trichloroacetic acid and held for drying. Dried cell plates were dyed for 30 min, after which the excess dye was washed away with 1% acetic acid. In a 10 mM tris base solution, the protein bound dye was dissolved. In a Varioskan flash Multimode reader, the OD was measured at 510 nm (Thermo Scientific) [24].

RESULTS AND DISCUSSION

Phytochemical analysis

The phytochemical evaluation of aqueous and ethanolic tuber extracts showed the presence of phenols, flavonoids, terpenoids, saponins, carbohydrates, and amino acids.

GC–MS analysis

Table 1 shows the results of GC–MS analysis of ethanolic tuber extract, which revealed a total 16 compounds. These compounds were identified using the NIST library and information from the literature. Some of the compounds had simple ring structures similar to those seen in the literature, but they varied in that they had different functional groups. The compounds were classified using retention time (RT), molecular structure, and peak area percentage. Fig. 1 depicts the GC–MS spectrum. Flavone, E, E, Z-1, 3, 12-nonadecatriene 5,14-diol, Phytol, and Methyl-6-octadecenoate were the major compounds in ethanolic tuber extract. The RTs with relative peak areas of the compounds were 17, 19.52, 18.68, and 18.9 min, with relative peak areas of 50%, 41.8%, 41.4%, and 40.2%, respectively [25-28].

Synthesis of AgNPs

The formation of AgNPs was primarily indicated by a transition in the color of the solution from light yellow to golden yellow. The presence of color in the reaction mixture was caused by mutual oscillations of electron-free conduction induced by an interacting electromagnetic field [29]. Noble metals were found to have unique optical properties due to the surface plasmon resonance (SPR), which indicates the synthesis of AgNPs by reducing silver metal ions Ag^+ into AgNPs Ag^0 by the active phytoconstituents present in the RTTE [30]. UV–Vis spectroscopy was used to screen the reduction process (Fig. 2a).

Effect of reaction time

The reaction time (Fig. 2b) was optimized by maintaining the reaction mixtures at room temperature and continuously observed. The samples were taken at regular intervals and analyzed using UV–Vis spectroscopy. Variations in reduction potentials were more likely to be responsible for the slower reduction rate of silver ions at room temperature. The redox potential for Ag^+ to Ag^0 was significantly smaller. After 24 h,

Table 1: Bioactive compounds detected in the ethanolic tuber extract of *R. tuberosa* by GC–MS

RT	Compound name	Molecular formulae	Molecular weight	% peak area	Type of compound
7.13	Cyclohexane, 3-(1-methyl ethyl)-	$C_{10}H_{20}$	140	11.2	Terpene
12.65	3-Cyclohexane -1-ol, 4-methyl1-(1-methylethyl)-	$C_{10}H_{18}O$	154	9.5	Terpene
14.17	α-Pinene	$C_{10}H_{16}$	136	8.8	Terpene
15.92	Phenol 2,4-bis (1,1-dimethyl ethyl)-	$C_{14}H_{22}O$	206	8.4	Phenolic compound
17	Flavone	$C_{15}H_{10}O_2$	222	50	Flavonoid
17.7	n-Hexadecanoic acid	$C_{16}H_{32}O_2$	172	24.2	Palmitic acid
18.68	Phytol	$C_{20}H_{40}O$	296	41.4	Diterpene
18.9	Methyl-6-octadecenoate	$C_{19}H_{36}O_2$	296	40.2	Stearic acid
9.52	E, E, Z-1,3,12-nonadecatriene5,14-diol	$C_{19}H_{36}O_2$	294	41.8	Terpene alcohol
20.17	Coumarin, 3-(2-[1-methyl-2-imidazolylthio]-1-oxoethyl)	$C_{15}H_{12}N_{20}3S$	300	24.3	Coumarin
20.52	Oleic acid	$C_{18}H_{34}O_2$	282	25.2	Fatty acid
21.4	Morin	$C_{15}H_{10}O_7$	302	16.4	Flavonoid
22.05	(E)-13-docosenoic acid	$C_{22}H_{42}O_2$	338	20.9	Fatty acid
22.85	1H-pyrolo (2,3-b) quinoxalin-2-imine, 2,3,3a, 4,9,9a-hexahydro-1, N-diphenyl-	NA	NA	11.3	Alkaloid
24.8	Phenol, 2,2-methylene bis (6-[1,1-dimethyl ethyl]-4-ethyl	$C_{25}H_{36}O_2$	368	6.5	Phenolic compound
27.47	4-piperidine acetic acid, 1-acetyl-5-ethyl-2-(3-[2-hydroxyethyl]-1 H-indol-2-yl)-a-methyl-, methyl ester	NA	NA	5.1	Alkaloid

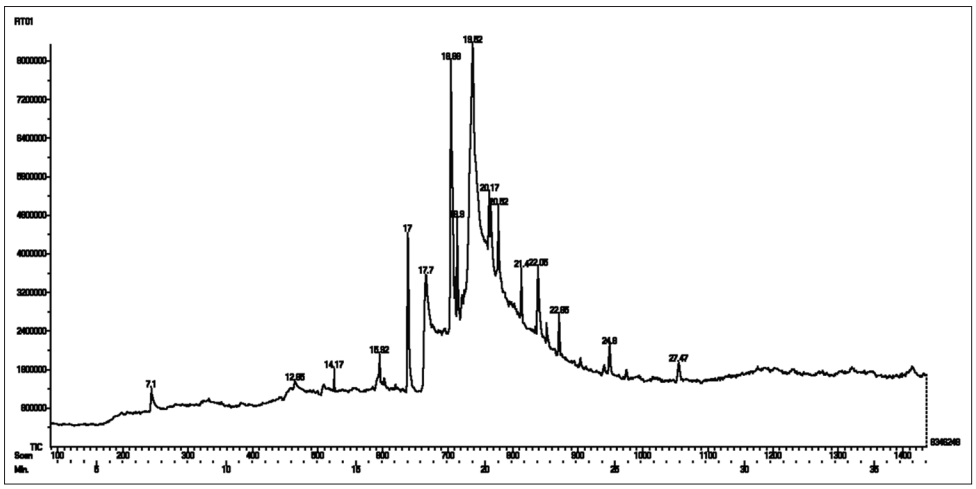

Fig. 1: Gas chromatography–mass spectrometry spectrum of ethanolic tuber extract of *Ruellia tuberosa*

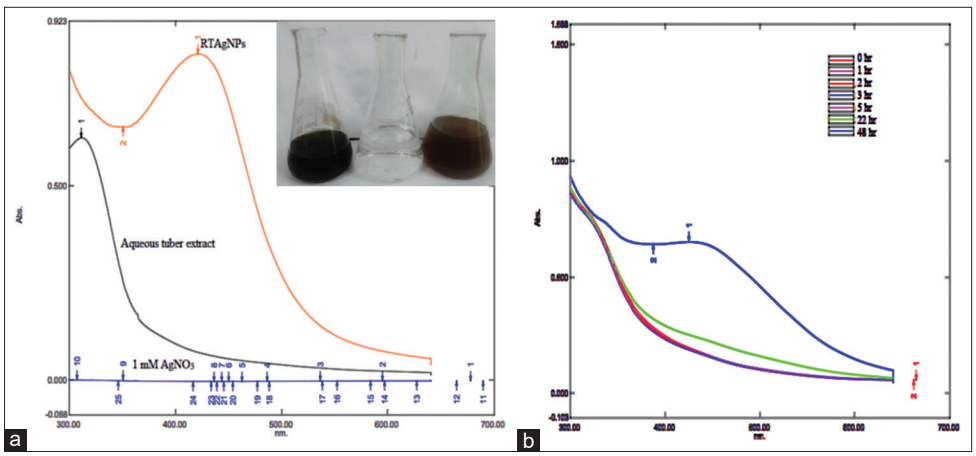

Fig. 2: (a) Ultraviolet–visible spectra of *Ruellia tuberosa*-mediated silver nanoparticle synthesis, (b) effect of time on silver nanoparticle synthesis for 1:8 ratio

AgNPs formed with less color intensity and fewer nanoparticles. Basing on the redox potential of plants, the time required for the completion of the reaction ranged from minutes to hours [23].

Effect of temperature

The temperature had an effect on the reduction process as well. The optimized reaction mixtures containing test tubes were kept in a water

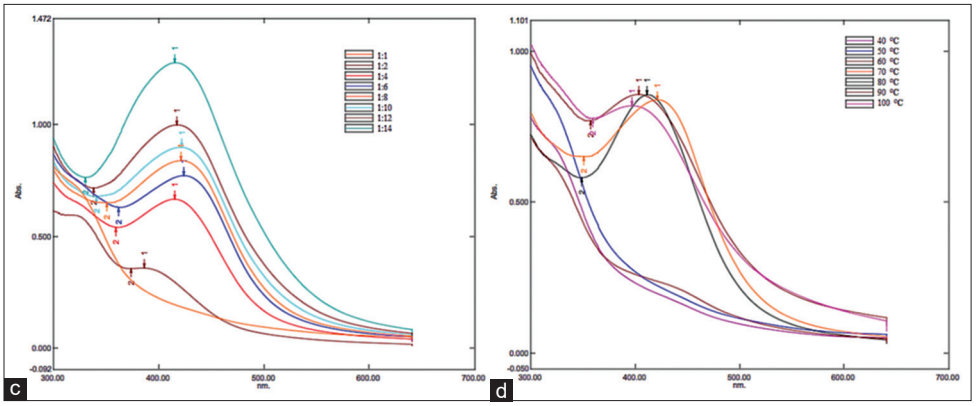

Fig. 2: (c) Different *Ruellia tuberosa* aqueous tuber extract to silver nitrate ratios at 70°C, (d) 1:8 at different temperatures

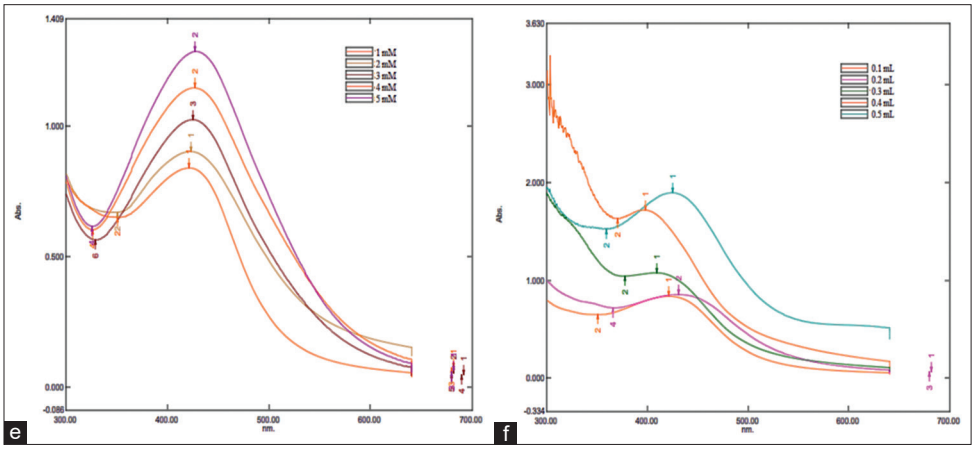

Fig. 2: (e) Effect of silver nitrate concentration, (f) effect of different volumes of aqueous tuber extract

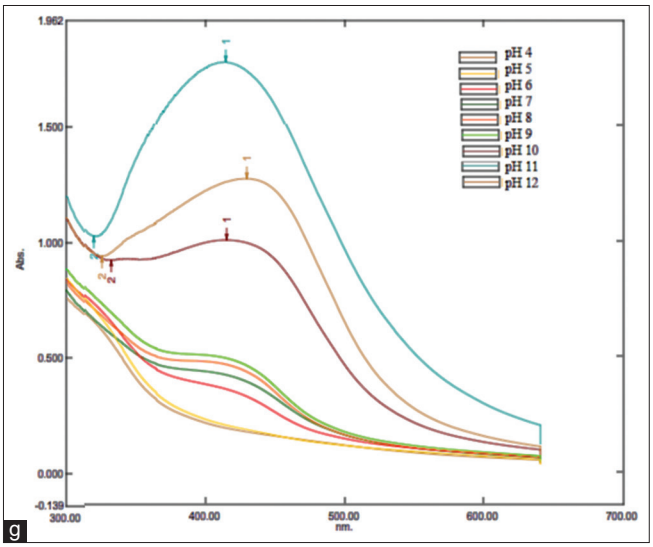

Fig. 2: (g) Effect of pH on silver nanoparticles synthesis

bath with an interval of 10°C rise in temperature at 40°, 50°, 60°, 70°, 80°, 90°, and 100°C. At 40–60°C, no noticeable rise in size or number of AgNPs was detected. At higher incubation temperatures (70–100°C), an increase in color intensity and more intense SPR peaks were revealed. The maximum SPR peak was detected at 421 nm at 70°C for 40 min [31]. Narrow peaks developed the smaller sized nanoparticles in the lower wavelength area (397 nm at 100°C) as the temperature was increased (Fig. 2c and d). When the temperature was raised, the reactants were quickly absorbed, resulting in the production of smaller nanoparticles [32,33].

Effect of metal salt concentration

At 0.1 mL of RTTE and 0.8 mL of $AgNO_3$ at 70°C for 40 min, the effect of $AgNO_3$concentration on AgNPs biosynthesis was monitored in the range of 1–5 mM. The SPR peaks for AgNPs at various metal ion concentrations are shown in Fig. 2e. For the specified reaction time, the color of the reaction mixture darkened as the concentration of $AgNO_3$ in the solution increased. According to the previous research studies, the size of nanoparticles was closely related to the color of the reaction mixture [33,34]. The number of synthesized AgNPs per unit volume of the reaction mixture increased with the band intensity increased. As a result, 1 mM $AgNO_3$ was chosen as the optimum concentration for achieving smaller particle sizes and stable growth [35].

Effect of crude aqueous tuber extract concentration

The aqueous tuber extract concentration was optimized by varying the RTTE volumes from 0.1 mL to 0.5 mL, while the other parameters were kept constant (temperature and concentration of $AgNO_3$). The number of nanoparticles was found to be greater in 0.2 mL of RTTE than in 0.1 mL. This increased nucleation at a higher reductant volume would result in a more significant number of nanoparticles and a more intense SPR band. When RTTE volume was increased from 0.3 to 0.5 mL (Fig. 2f), the SPR band becomes more prominent and less concentrated with a blue shift in wavelength. Since there was more reductant available than free Ag^+ ions for the growth of stable nuclei, the reaction rate increased, resulting in a more significant number of small-sized nanoparticles [33,36].

Effect of pH

pH influenced the shape, size, and stability of the AgNPs. These three different buffer solutions were used to carry out the reactions, ranging

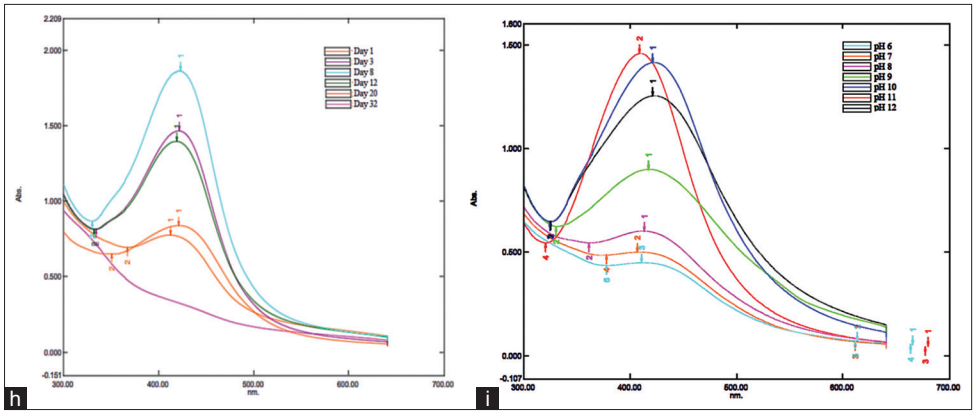

Fig. 2: (h) Stability of synthesized silver nanoparticles, (i) stability in the presence of polyvinylpyrrolidine

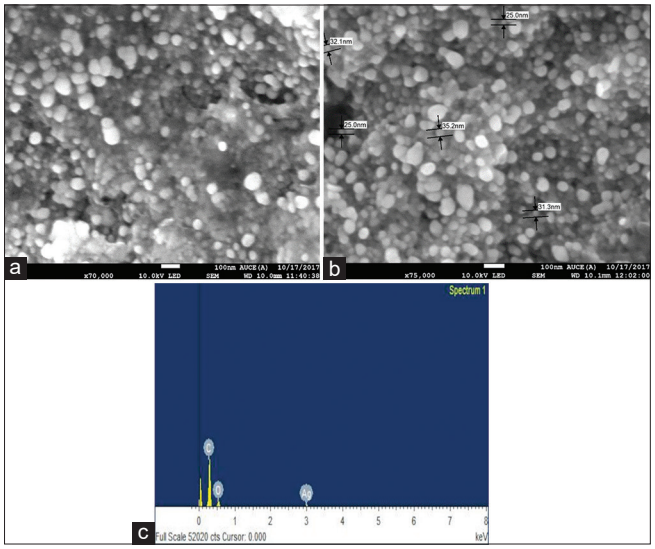

Fig. 3: (a and b) Field emission scanning electron microscopy images of RT silver nanoparticles, (c) corresponding energy-dispersive X-ray spectroscopy spectrum of silver nanoparticles

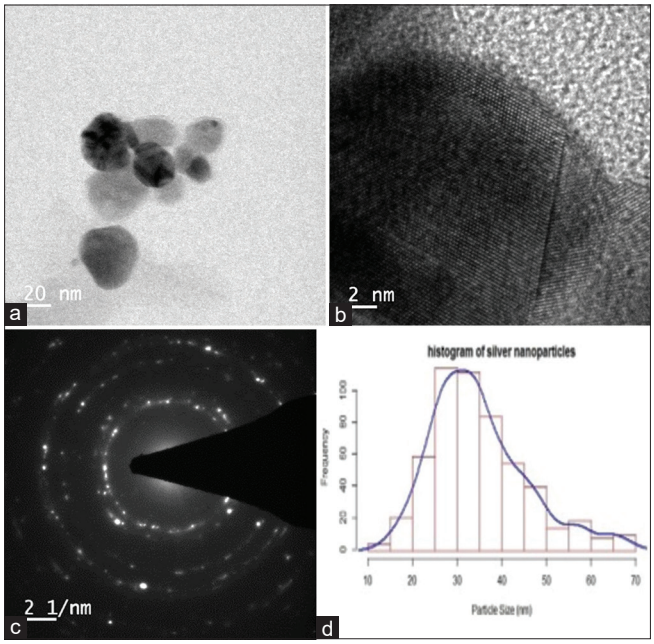

Fig. 4: (a and b) High-resolution transmission electron microscope micrographs of the silver nanoparticles, (c) selected area electron diffraction pattern showing the characteristic crystal planes of elemental silver, (d) particle size distribution histogram

the pH from 4 to 12. Tris HCl (7, 8, 9), phosphate buffer (4, 5, 6), and glycine-NaOH (10,11,12) [37]. There was no color transition or characteristic SPR peak in acidic conditions. When the solution becomes more alkaline, the color intensity increased from dark yellow to reddish- orange. The development of AgNPs was instantaneous at alkaline pH, and an extreme SPR peak was observed at pH11 (Fig. 2g). At higher pH, alkalinity promoted AgNPs reduction and capping at various facets and the eventual accumulation of silver atoms on these facets [38]. However, because of the high concentration of hydrogen ions, the functional groups responsible for reducing the precursor to nanoparticles had positive charges at acidic pH, lowering their reducing potential.

Stability studies

AgNPs synthesized from the optimum reaction mixture (1 mL of RTTE in 8 mL of 1 mM $AgNO_3$) were studied for stability at 70°C for 40 min, as shown in Fig. 2h. The visual precipitation and the shift in SPR peak intensity were all taken into consideration when examining the stability of AgNPs. Even 4 weeks after their synthesis, the AgNPs were shown to be stable in solution [23]. The particles remained stable for 95 days at 4°C. Following that, AgNPs precipitation was found at the tube's bottom, attributed to AgNP overgrowth and agglomeration overtime.

To compare the stability of biologically synthesized nanoparticles, a stabilizing agent like polyvinylpyrrolidone (PVP) (0.2% and 0.5%) aqueous solution was used at pH 5. PVP concentration significantly influenced the size distribution as well as the dispersion of the resulting nanoparticles. Particles were stable for up to 45 days at room temperature (Fig. 2i), AgNPs were stable for more than 6 months at 4°C. PVP was considered an excellent dispersant as it possess favorable protected properties. At low PVP concentration, some agglomerated particles were observed. However, when the PVP concentration was increased (0.5%), well isolated with controlled size and monodispersed nanoparticles were formed. Therefore, PVP regulated bond formation between individual AgNPs and protected the particles from agglomeration by forming a layer of the stabilizing agent on the surface of nanoparticles [39].

Characterization of AgNPs

FESEM analysis

FESEM was used to analyze the shape of the synthesized AgNPs. A powdered AgNPs sample was used for the analysis. An agglomeration of nanoparticles was visible in the FESEM image (Fig. 3a and b). The nanoparticles were formed spherical and polydispersed. The purity and elemental composition of AgNPs were determined using an EDX detector connected with a FESEM. According to the energy-dispersive spectrum

image, the nanoparticle was mainly composed of silver (Fig. 3b). In EDX spectra, a silver peak recorded at 3 keV. Apart from silver signal, spectral signals for oxygen and carbon were also observed [40]. Carbon spectra had the most prominent peak due to the carbon sheet on which the sample smear was made [41]. Gardea-Torresdey *et al*. used alfalfa (*M. sativa*) plant to form individual spherical-shaped AgNPs in the range of 2.5–4 keV [7].

HRTEM analysis

HRTEM data were used to investigate the detailed surface morphology of biosynthesized AgNPs. The HRTEM image (Fig. 4a and b) showed many nearly spherical AgNPs ranging in size from 11.6 nm to 69.7 nm. The onset of Fig. 4c showed the selected area electron diffraction (SAED) sequence of AgNPs. The bright circular rings indicated the crystalline nature of synthesized AgNPs in the SAED pattern. A size distribution histogram defined the average size distribution of nanoparticle (34.9 nm) (Fig. 4d), which was derived from many micrographs of AgNPs corresponding to HRTEM images. Similar findings were observed in the synthesis of AgNPs mediated through mangosteen (*Garcinia mangostana*) leaf extract with an average size of 35 nm [36].

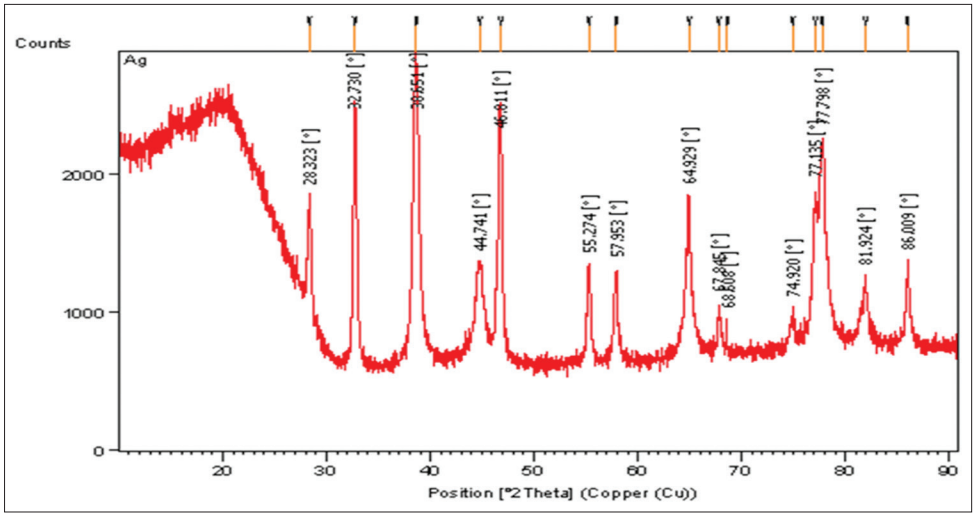

Fig. 5: X-ray diffractogram of *Ruellia tuberosa* tuber mediated silver nanoparticles

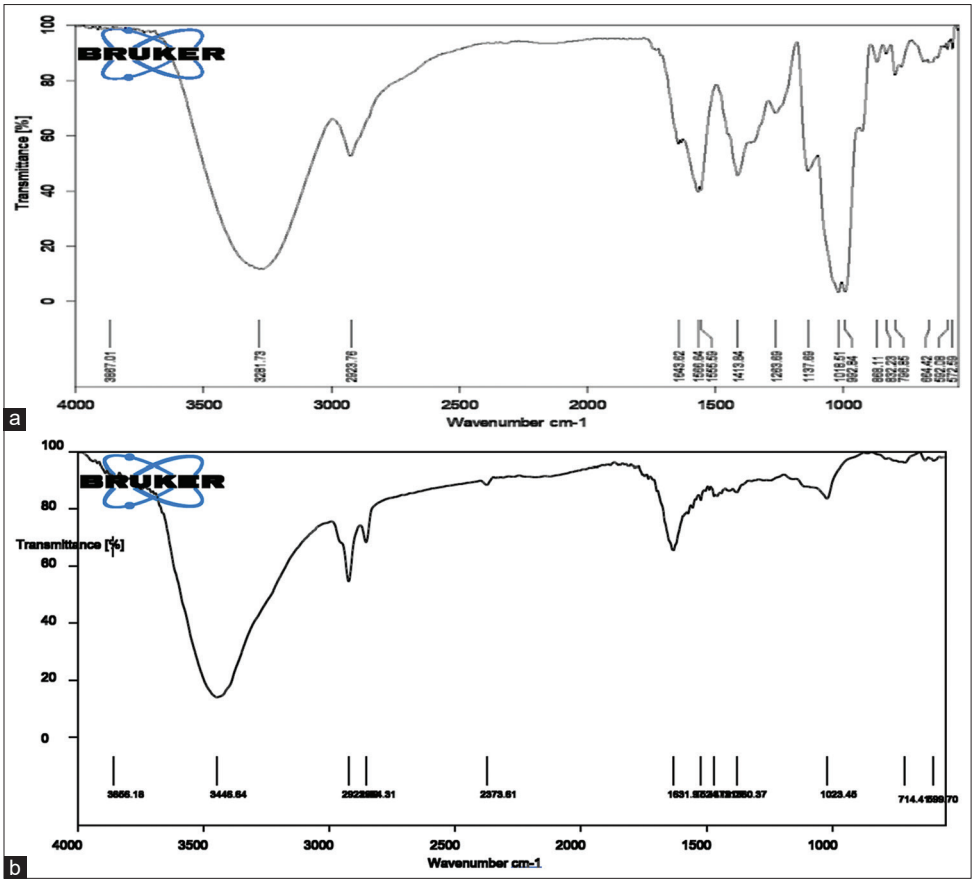

Fig. 6: Fourier transform infrared spectra of (a) *Ruellia tuberosa* aqueous tuber extract, (b) retention time tuber mediated silver nanoparticles

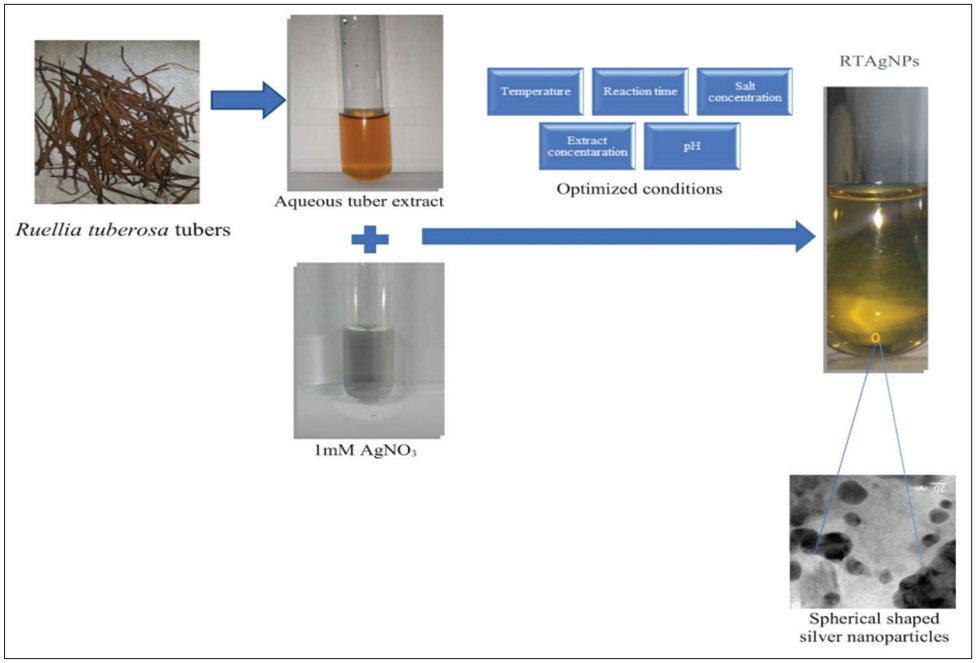

Fig. 7: Possible mechanism of silver nanoparticles synthesis from *Ruellia tuberosa* aqueous tuber extract

XRD analysis

Fig. 5 shows XRD data of synthesized AgNPs obtained over a broad angular range of 20°≤2θ≤80°, revealed the crystalline structure of AgNPs. The XRD pattern of AgNPs revealed that four prominent distinct diffraction peaks at 2θ=38.65°, 44.74°, 64.92°, and 77.79°, which correspond to the (111), (200), (220), and (311) were similar with those recorded for the standard silver metal (Ag°) Joint Committee on Power Diffraction Standards (JCPDS No. 00-04-0783, USA). By comparing the JCPDS values, the typical pattern of green synthesized AgNPs was found to possess a face-centered cubic (FCC) structure [9-11]. Additional unassigned peaks were found in addition to the Bragg peaks representative of FCC silver nanocrystals, implied that bio-organic phase crystallization occurred on the surface of the AgNPs. The average crystallite size of the synthesized AgNP was determined using the Debye Scherrer equation.

$$D=K\lambda/\beta \cos \theta \quad (1)$$

Where, D is the average particle size, k is the shape factor (constant 0.9), λ is the X-ray wavelength (1.5406A°), β is the full width at half maximum of the peak, and θ is the diffraction angle. The average crystallite size of the AgNP synthesized by aqueous tuber extract of *R. tuberosa* was arrived at 39.8 nm, which was nearer to TEM size.

FTIR analysis

The possible biomolecules in RTTE responsible for the synthesis and stabilization of AgNPs were investigated using FTIR analysis of both RTTE and AgNPs. RTTE had notable bands at 3281.73, 2923.76, 1643.62, 1566.64, 1413.84, 1137.69, and 1018.51 cm^{-1} in its IR spectra (Fig. 6a). The band at 3281 cm^{-1} represents -OH groups of tannins, flavonoids (phenolic compounds), glucose, and –NH stretching of proteins [10,42]. A band at 2923.76 cm^{-1} correlates to –C–H asymmetric stretching of alkanes, 1643.62 cm^{-1} to C=O of carbonyl group. Bands at 1566.64, 1555.59, and 1413.84 cm^{-1} to C-O-C stretching of alkene functional groups, and band at 1018.51 cm^{-1} to –C–O stretching vibrations of ether and alcoholic groups, respectively [11,43]. In contrast to the IR spectrum of RTTE, the spectra of AgNPs showed a change in the following peaks: From 3281.73 to 3446.64, 2923.76 to 2923.40, 1643.62 to 1631.97, 1555.59 to 1524.19, and 1413.84 to 1472.07, 1018.51 to 1023.45 cm^{-1} (Fig. 6b). According to these results, the hydroxyl, carboxyl, amino, and amide groups of biomolecules present in RTTE served as reducing and capping agents for the biosynthesis of AgNPs. Flavonoids, phenolic compounds, tannins, carbohydrates, and amino acids found in RTTE may contribute to these groups [44].

Possible mechanism of AgNPs formation

The exact process by which plants produce nanoparticles was unknown. Phenolics, flavonoids, terpenoids, sugars, and amino acids were among the phytochemical constituents contained in the aqueous tuber extract [44]. These compounds could help to reduce metal salt solutions (Ag^+ to Ag°) and act as capping agents, resulted in stable AgNPs. The formation and size of nanoparticles were effected by several optimization parameters (Fig. 7).

Antiproliferative activity

No significant results were observed after performing the *in vitro* antiproliferative activity on A549, HeLa, MDA-MB 231, PANC-1, and SK-OV-3 cell lines.

CONCLUSION

In this study, AgNPs were synthesized using a crude aqueous tuber extract of *R. tuberosa*. GC–MS data revealed that the tuber of *R. tuberosa* was rich in various phytochemical constituents. These phytochemicals could aid in nanoparticle synthesis by acting as reducing and capping agents. After studying the effect of various physicochemical parameters, the optimized conditions were found to be 0.1 mL aqueous tuber extract, 1 mM $AgNO_3$ at 70°C, at pH 11. These particles were stable for up to 4 weeks. AgNPs synthesized by *R. tuberosa* were spherical in shape and crystalline in nature, with an average particle size of 34.9 nm.

ACKNOWLEDGMENT

The authors gratefully acknowledge Advanced Analytical Laboratory (DST) and Centre for Nanotechnology, Andhra University College of Engineering, Andhra University, Visakhapatnam, for providing XRD and FESEM data. We were also thankful to SAIF, IIT, Madras, and IIT, Bombay, for providing GC–MS and HRTEM data.

AUTHORS' CONTRIBUTIONS

N.L.C. Harika M: Investigation, original draft preparation (half), Radhika P: Conceptualization, supervision, resources, review, and editing (half).

CONFLICTS OF INTEREST

The authors declare that they have no known competing financial interest that could have influenced the work reported in this paper.

FUNDING INFORMATION

Thanks are due to financial support provided by UGC, New Delhi (Ref. No. 42-376/2013 [SR]), for a period of 3 years (2013–2017).

REFERENCES

1. Chhangte V, Samuel L, Ayushi B, Manickam S, Bishwajit C, Samuel LR. Green synthesis of silver nanoparticles using plant extracts and their antimicrobial activities: A review on recent literature. RSC Adv 2021;11:2804-37.
2. Nadeem B, Irshad K, Wail F. Nanomaterials: A review of synthesis methods, properties, recent progress, and challenges. Mater Adv 2021;2:1821-71.
3. Marryam M, Mehwish A, Muhammad FN, Muhammad NZ, Muhammad AR, Muhammad A, *et al.* The wet chemical synthesis of surfactant-capped quasi-spherical silver nanoparticles with enhanced antibacterial activity. Mater Adv 2020;1:2332-8.
4. Rizwan A, Rahis U. A review on recent developments in the biosynthesis of silver nanoparticles and its biomedical applications. Med Devices Sens 2021;4:1-20.
5. Dan Z, Ma XL, Gu Y, Huang H, Guang-Wei Z. Green synthesis of metallic nanoparticles and their potential applications to treat cancer. Front Chem 2020;8:1-18.
6. Hussain M, Raja NI, Iqbal M, Aslam S. Applications of plant flavonoids in the green synthesis of colloidal silver nanoparticles and impacts on human health. Iran J Sci Technol Trans A Sci 2019;43:1381-92.
7. Gardea-Torresdey JL, Gomez E, Peralta-Videa JR, Parsons JG, Troiani HE, Jose-Yacaman M. Alfalfa sprouts: A natural source for the synthesis of silver nanoparticles. Langmuir 2003;19:1357-61.
8. Remya V, Siby J, Beena M. *Indigofera tinctoria* leaf extract mediated green synthesis of silver and gold nanoparticles and assessment of their anticancer, antimicrobial, antioxidant and catalytic properties. Artif Cell Nanomed Biotechnol 2018;46:861-71.
9. Nataya S, Siriluck A, Surang N. Larvicidal activity of synthesized silver nanoparticles from *Curcuma zedoaria* essential oil against *Culex quinquefasciatus*. Insects 2019;10:1-11.
10. Sharifi-Rad M, Pawel P, Francesco E, Álvarez-Suarez JM. Green synthesis of silver nanoparticles using *Astragalus tribuloides* Delile. Root extract: Characterization, antioxidant, antibacterial, and anti-inflammatory activities. Nanomaterials 2020;1:1-17.
11. Aishah MY, Azieyan CM, Ahmad NH, Doblin S, Chee KL, Lim V. Optimization of biogenic synthesis of silver nanoparticles from flavonoid rich *Clinacanthus nutans* leaf and stem aqueous extracts. R Soc Open Sci 2020;7:20006.
12. Majid SJ, Aya AH, Ghassan MS, Nahi YY, Yaser HD Mona SA, *et al.* Green synthesis of silver nanoparticles from *Eriobotrya japonica* extract: A promising approach against cancer cells proliferation, inflammation, allergic disorders and phagocytosis induction. Artif Cell Nanomed Biotechnol 2021;49:48-60.
13. Nancy J, Priyanshu J, Devyani R, Umesh Kumar P. Green synthesized plant-based silver nanoparticles: Therapeutic prospective for anticancer and antiviral activity. Micro Nano Syst Lett 2021;9:1-24.
14. Kishore S, Radhika P. Review on the antimicrobial and anticancer properties of noble metal nanoparticles synthesized using variety of plant extracts: A green strategic approach. Res J Biotechnol 2016;11:136-58.
15. Lans CA. Ethnomedicines used in Trinidad and Tobago for urinary problems and diabetes mellitus. J Ethnobiol Ethnomed 2006;2:1-11.
16. Rajendrakumar N, Vasantha K, Murugan M, Mohan VR. Antioxidant activity of tuber of *Ruellia tuberosa* L. Int J Pharmacogn Phytochem Res 2014;6:97-103.
17. Bhogaonkar PY, Kanerkar UR, Indurwade NH, Chondekar RP. Antispermatogenic effect of the aqueous root extracts of *Ruellia tuberosa* L. On albino rats. Trends Life Sci 2012;1:1-4.
18. Rajendrakumar N, Vasantha K, Nishanthini A, Mohan VR. Anti-inflammatory activity of tubers of *Ruellia tuberosa* L. (*Acanthaceae*). World J Pharm Pharm Sci 2014;3:1371-5.
19. Kader AM, Parvin S, Chowduri AM, Haque EM. Antibacterial, antifungal and insecticidal activities of *Ruellia tuberosa* (L) root extract. J Biosci 2012;20:91-7.
20. Vasantharaj S, Selvam S, Palanisamy S, Felix LO, Arivalagan P. Biosynthesis of iron oxide nanoparticles using leaf extract of *Ruellia Tuberosa*: Antimicrobial properties and their applications in photocatalytic degradation. J Photochem Photobiol B Biol 2019;192:74-82.
21. Vasantharaj S, Selvam S, Sripriya NS, Jaya Ganesh TN, Pannerselvam B, Al-Misned FA, *et al*. Cytotoxic effects of silver nanoparticles on *Ruellia tuberosa*: Photocatalytic degradation against cystal violet and coomasie brilliant blue. J Environ Che Eng 2021;9:1-9.
22. Trease EG, Evans WC. Text Book of Pharmacognosy. 14th ed. United Kingdom: WB Saunders Company;1997. p. 119.
23. Shankar SS, Rai A, Ahmad A, Sastry M. Rapid synthesis of Au, Ag, and bimetallic Au core-Ag shell nanoparticles using neem (*Azadirachta indica*) leaf broth. J Colloids Interf Sci 2004;275:496-502.
24. Vanicha V, Kanyawim K. Sulforhodamine B colorimetric assay for cytotoxicity screening. Nat Protoc 2006;1:1112-6.
25. Srinivasan K, Sivasubramanian S, Kumaravel S. Phytochemical profiling and GCMS study of *Adhathoda vasica* leaves. Int J Pharm Bio Sci 2014;5:714-20.
26. Kumar A. Chemical composition of essential oil isolated from the rhizomes of *Kaempferia galanga* L. Int J Pharm Bio Sci 2014;5:225-31.
27. Arul Priya R. Saravanan K. Phytochemical and GC-MS studies of traditional herbaceous plant pumpkin (*Cucurbita pepo*) L. J Cell Tissue Res 2017;17:6035-41.
28. Karthikeyan V, Baskaran A, Sebastian Rajasekaran C. Gas chromatography-mass spectroscopy (GC-MS) analysis of ethanolic extracts of *Barleria acuminata* Nees. Int J Pharmacol Res 2016;6:55-61.
29. Mulvaney P. Surface plasmon spectroscopy of nanosized metal particles. Langmuir 1996;12:788-800.
30. Ahmad A, Mukherjee P, Senapati S, Mandal D, Khan MI, Kumar R, *et al*. Extracellular biosynthesis of silver nanoparticles using the fungus *Fusarium Oxysporum.* Colloids Surf B 2003;28:313-8.
31. Sri Ramkumar V, Prakash S, Muthukkumarasamy S, Natarajan Kumari A, Ravindran J, Kannapiran E. Synthesis and characterization of silver and gold nanoparticles using aqueous extract of seaweed, *Turbinaria conoides*, and their antimicrofouling activity. Sci World J 2014;2014:1-10.
32. Park J, Joo J, Kwon SG, Jang Y, Hyeon T. Synthesis of monodisperse spherical nanocrystals. Angew Chem 2007;46:4630-60.
33. Jae YS, Beom SK. Rapid biological synthesis of silver nanoparticles using plant extracts. Bioprocess Biosyst Eng 2009;32:79-84.
34. Mock JJ, Barbic M, Smith DR, Schultz DA, Schultz S. Shape effects in plasmon resonance of individual colloidal silver nanoparticles. J Chem Phys 2002;116:6755-9.
35. Pimprikar PS, Joshi SS, Kumar AR, Zinjarde SS, Kulkarni SK. Influence of biomass and gold salt concentration on nanoparticle synthesis by the tropical marine yeast *Yarrowia lipolytica* NCIM 3589. Colloids Surf B Biointerf 2009;74:309-16.
36. Ravichandran V, Xin TZ, Subhashini G, Xiang TF, Yang EF, Jeyakumar N, *et al*. biosynthesis of silver nanoparticles using Mangosteen leaf extract and evaluation of their antimicrobial activities. J Saudi Chem Soc 2011;15:113-20.
37. Semra C, Azize Alayl JG, Ahmet A, Hayrunnisa N. Biochemical evaluation and green synthesis of nano silver using peroxidase from *Euphorbia* (*Euphorbia amygdaloides*) and its antibacterial activity. J Che 2015;1-7.
38. Maria BS, Aishwarya D, Vidya Shetty K, Saidutta MB. Synthesis of silver nanoparticles using medicinal *Zizyphus xylopyrus* bark extract. Appl Nanosci 2015;5:755-62.
39. Malina D, Sobczak-Kupiec A, Wzorek Z, Kowalski Z. Silver nanoparticles synthesis with different concentrations of polyvinylpyrrolidone. Dig J Nanomater Bios 2012;7:1527-34.
40. Jayaseelan C, Ramkumar R, Rahuman AA, Perumal P. Green synthesis of gold nanoparticles using seed aqueous extract of *Abelmoschus esculentus* and its antifungal activity. Ind Crop Prod 2013;45:423-9.
41. Sridhar S, Rakesh KM, Satish K, Mitali M, Arnab G, Mrutyunjay S, *et al*. Polysaccharide-capped silver nanoparticles inhibit biofilm formation and eliminate multidrug-resistant bacteria by disrupting bacterial cytoskeleton with reduced cytotoxicity towards mammalian cells. Sci Rep 2016;6:1-16.
42. Roopan SM, Rohit, Madhumitha G, Rahuman AA, Kamaraj C, Bharathi, *et al*. Low-cost and ecofriendly phyto-synthesis of silver nanoparticles using *Cocos nucifera* coir extract and its larvicidal activity. Ind Crop Prod 2013;43:631-5.
43. Socrates G. Infrared Characteristic Group Frequencies. New York: Wiley-Interscience Publication; 1980.
44. Supawana K, Supawatchara S, Sastraruji T, Jaikang C. Phytochemical study of *Ruellia tuberosa* chloroform extract: Antioxidant and anticholinesterase activities. Der Pharm Lett 2016;8:238-44.